Thermochimica Acta, 113 (1987) 79–86
Elsevier Science Publishers B.V., Amsterdam – Printed in The Netherlands

CHANGES IN TEXTURAL PROPERTIES DERIVED FROM THE THERMAL DECOMPOSITION OF SYNTHETIC PYROAURITE

M.A. ULIBARRI and M.J. HERNANDEZ

Departamento de Química Inorgánica, Facultad de Ciencias, Universidad de Córdoba (Spain)

J. CORNEJO *

Instituto de Recursos Naturales y Agrobiología, C.S.I.C. Aptdo. 1052, Sevilla (Spain)

(Received 28 July 1986)

ABSTRACT

Pyroaurite has the formula $Mg_{6.056}Fe_{1.944}(OH)_{16}(CO_3)_{0.968}\cdot 3.912\ H_2O$, and has been hydrothermally synthesized. The thermal decomposition of this layered double hydroxy-carbonate was followed by differential thermal analysis and thermogravimetric analysis, and the reaction products have been studied by X-ray powder diffraction, scanning electron microscopy and N_2-adsorption techniques. A scheme for the thermal decomposition of pyroaurite is suggested. Three stages may be differentiated during the course of the reaction: (a) interlayer water was lost around 200°C; (b) CO_2 was released from the interlayer region as well as H_2O from the brucite-like layer at 300–450°C; and (c) at higher temperatures, 600–1000°C, a mixture of MgO and the spinel, $MgFe_2O_4$, was formed. Changes in BET surface area, porosity and morphology of synthetic pyroaurite under heat treatment are discussed.

INTRODUCTION

Pyroaurite and sjögrenite are two polymorphs of typical composition $[Mg_6Fe_2(OH)_{16}](CO_3)\cdot 4H_2O$. These minerals typify an extensive group of natural and synthetic compounds expressed by the formula $[M^{2+}_{1-x}M^{3+}_x(OH)_2]^{x+}\ X^{m-}_{x/m}\cdot nH_2O$, where $M^{2+} = Mg^{2+}$, Ni^{2+}, Fe^{2+}, etc. $M^{3+} = Al^{3+}$, Fe^{3+}, Cr^{3+}, etc., and $X^{m-} = CO_3^{2-}$, SO_4^{2-}, NO_3^-, Cl^-, etc. [1–3]. The structure of these materials consists of a repetition of brucite-like layers, positively charged by substitution of M^{3+} for M^{2+}, and interlayers formed by anions and water molecules [4].

The thermal behaviour of some of these compounds has been studied and it was found that the interlayer water is reversibly removed at low temperatures, whilst at higher temperatures the interlayer anions are gradually

---

* Author to whom correspondence should be addressed.

0040-6031/87/$03.50

released and dehydroxylation occurs resulting in the formation of metallic oxides [5–9]. The dehydrated materials show a molecular sieving property and calcination yields highly active oxides [10]; however, little attention seems to have been paid to the study of the resultant products of the thermal decomposition [11].

In this paper, a detailed study of the resultant products of the thermal treatment of Mg, Fe hydroxycarbonate has been carried out using differential thermal analysis (DTA) and thermogravimetric analysis (TGA), X-ray powder diffraction (XRD), scanning electron microscopy (SEM) and nitrogen adsorption techniques.

EXPERIMENTAL

Mg, Fe hydroxycarbonate was synthesized by slow addition of an NaOH solution to a mixed and diluted solution of $MgCl_2$ and $FeCl_3$ with a Mg/Fe molar ration of 3/1, until a final pH of 10 was achieved. The mixture was vigorously stirred during the reaction and the resulting gel was hydrothermally treated for several days at about 130°C to improve crystallinity. The product was then washed to eliminate salt excess and dried at 60°C.

Mg and Fe were determined after dissolution of the solid in dilute HCl by atomic absorption spectrometry on a Perkin-Elmer 380 spectrometer. X-ray powder diffraction patterns were recorded on a Siemens D500 diffractometer using CuK_α radiation at a scanning rate of $1°2\theta$ min^{-1}.

TGA and DTA curves were obtained in a static air atmosphere at a heating rate of 10°C min^{-1} using a Rigaku-Thermoflex TG-DTA instrument.

Scanning electron micrographs were obtained by using a Philips SEM 501 B. Samples were gently dispersed by ultrasound in an acetone medium, settled on Ni holders and covered with an electrodeposited gold film.

Adsorption–desorption isotherms of N_2 were obtained at 77 K in a conventional volumetric apparatus. The samples were previously equilibrated in a vacuum (better than 10^{-4} mbar). Surface areas were calculated using the BET [12] and α_s-plot [13] procedures, assuming a cross-sectional area of 16.2 $Å^2$ for the N_2 molecule. Mesopore analysis was carried out using the methods of Dollimore and Heal [14] and Lippens et al. [15], assuming cylindrical and slit-shape geometries for the pores, respectively. The total pore volumes, V_p, were read directly from the isotherms at $P/P_0 = 0.95$.

RESULTS AND DISCUSSION

The XRD pattern of the synthetic pyroaurite (Fig. 1) shows all the spacings corresponding to this hydroxycarbonate [16]. The interlayer dis-

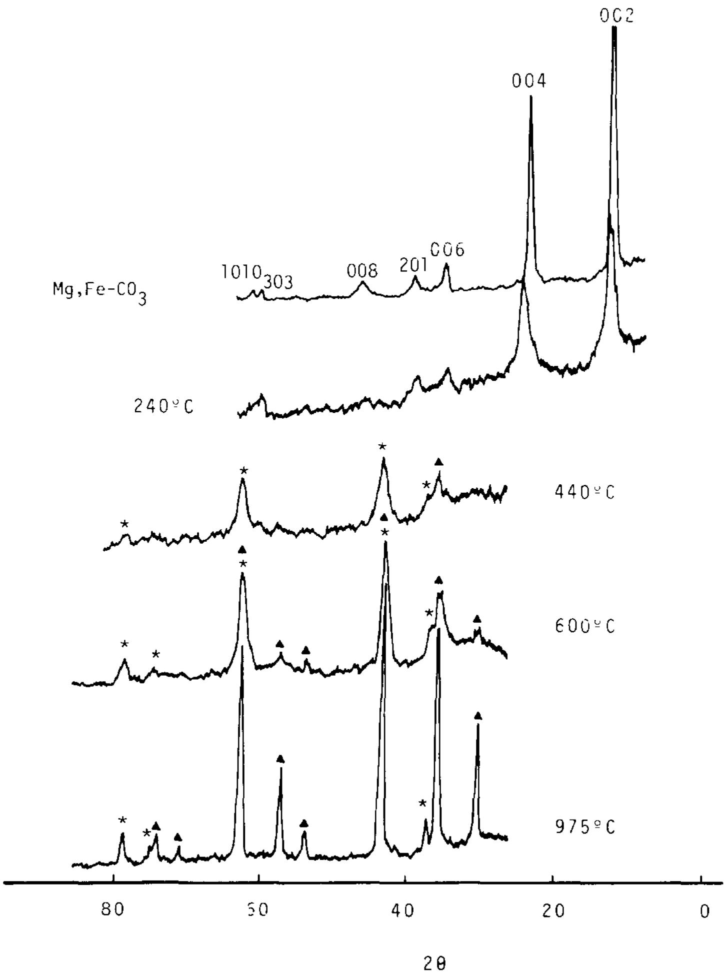

Fig. 1. X-ray powder diffraction patterns for Mg, Fe hydroxycarbonate untreated and after calcination at different temperatures: (*) MgO, (▲) $MgFe_2O_4$.

tance, c', corresponding to $c/2$ and obtained using the (002) reflection, 7.89 Å, is comparable with that of $c' = 7.805$ Å obtained by Allman [16] for natural pyroaurite. This layer spacing, c', is equal to the brucite-like layer plus the interlayer containing CO_3^{2-} ions and water molecules.

The thermal decomposition of the synthetic pyroaurite using TGA and DTA was similar to that of natural pyroaurite [17]. The corresponding TGA and DTA diagram is shown in Fig. 2 in which two main endothermic effects can be observed. According to the TGA data and the XRD diffraction pattern of the compound obtained after the first endothermic effect (200°C), this can be attributed to the elimination of the interlayer water. The XRD pattern of the compound heated at 240°C (Fig. 1) shows the spacings

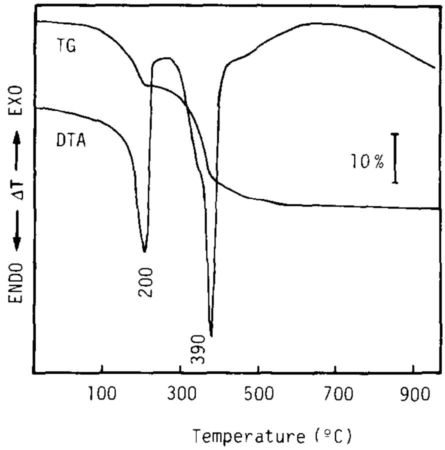

Fig. 2. DTA and TGA curves for Mg, Fe hydroxycarbonate.

corresponding to the laminar hydroxycarbonate with a slight diminution of the (001) reflections [7.89 to 7.75 Å for (002)]. At temperatures between 300 and 450 °C, two superimposed endothermic effects occurred, with a shoulder at 340 °C and a sharp peak at 380 °C. Both effects are related to the slow release of CO_2 from the interlayer region and the dehydration of the brucite-like layers. The X-ray diffractogram of the sample heated at 440 °C shows lines corresponding to poorly crystallized MgO and a peak which is ascribed to the maximum intensity of the spinal phase, indicating that the interaction between metallic oxides has begun. A very small endothermic effect can be observed at 490 °C which could be ascribed to the final dehydroxylatin of the sample. The TGA curve shows a weight loss between 300 and 600 °C corresponding to the above mentioned endothermic effects. At higher temperatures (600 °C) the XRD patterns show the main lines corresponding to the $MgFe_2O_4$ and at 975 °C all the spacings ascribed to the spinel and non-reacted, well-crystalline, MgO are observed, which indicates that, as expected, the increase in the calcination temperature improves the crystallinity of these compounds.

On the basis of the above results the following scheme can be proposed for the thermal decomposition of the synthetic pyroaurite:

$$Mg_{6.056}Fe_{1.944}(OH)_{16}(CO_3)_{0.968}\cdot 3.912\ H_2O$$

$$\xrightarrow{200\,^\circ C} Mg_{6.056}Fe_{1.944}(OH)_{16}(CO_3)_{0.968} + 3.912\ H_2O \xrightarrow{300\text{–}600\,^\circ C} 5.084\ MgO$$

$$+\,0.972\ MgFe_2O_4 + 0.968\ CO_2 + 8\ H_2O$$

In order to find out the effects of heating on the textural properties of this sample and its decomposition products, N_2 adsorption–desorption isotherms of the original sample (a), and samples treated at 600 °C (b) and 975 °C (c) are shown in Fig. 3. The curve corresponding to the untreated

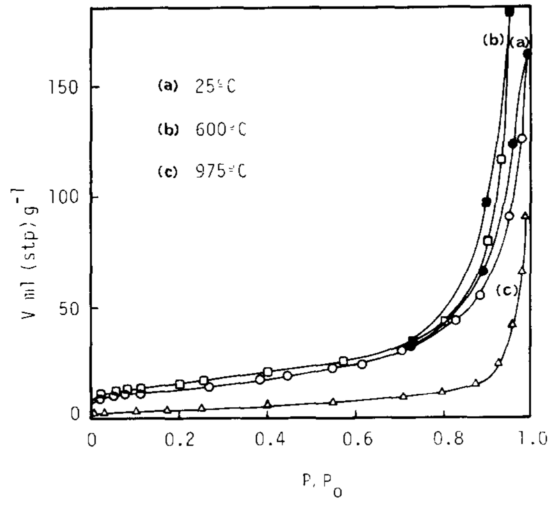

Fig. 3. N_2 adsorption isotherms at 77 K for Mg, Fe hydroxycarbonate. Empty symbols, adsorption; filled symbols, desorption.

sample, (a), can be considered as type II of the BDDT classification [18], whereas the 600°C (b) and 975°C (c) treated samples belong to type IV of this classification. The adsorption–desorption curves corresponding to treated samples at 150, 240, 440 and 800°C are not included in Fig. 3 for simplicity, but they are similar in shape to curves (b) and (c). The hysteresis loops have characteristics like those described as type H_3 in the IUPAC classification [19] which is often obtained when adsorbents having plate-like morphology, as shown in the corresponding SEM micrographs (Fig. 4).

The α_s-plots (not shown) have been constructed in the manner previously described by Sing [13]. The non-porous sample obtained by heating the original sample at 975°C and outgassed at room temperature was used as standard. A straight line passing through the origin was obtained at low relative pressure in every case. However, the corresponding α_s-plots exhibited a considerable upward deviation, indicating the absence of microporosity and capillary condensation.

Surface-area values, calculated by the BET and α_s methods (S_{BET} and S_α, respectively), are given in Table 1. Satisfactory agreement is observed between the corresponding S_{BET} and S_α values, indicating the correctness in the choice of the standard sample used in the α-plots. Cumulative surface areas, S_{cum} and S'_{cum} (Table 1) were obtained for mesoporous samples following the Dollimore and Heal [14] and Lippens et al. [15] methods, respectively. The t-values used in these analyses were obtained from the N_2-adsorption isotherm on the non-porous reference sample used as standard. S_{BET} (or S_α) values agree much better with the corresponding S_{cum} values than with the S'_{cum} values for the mesoporous samples studied. This

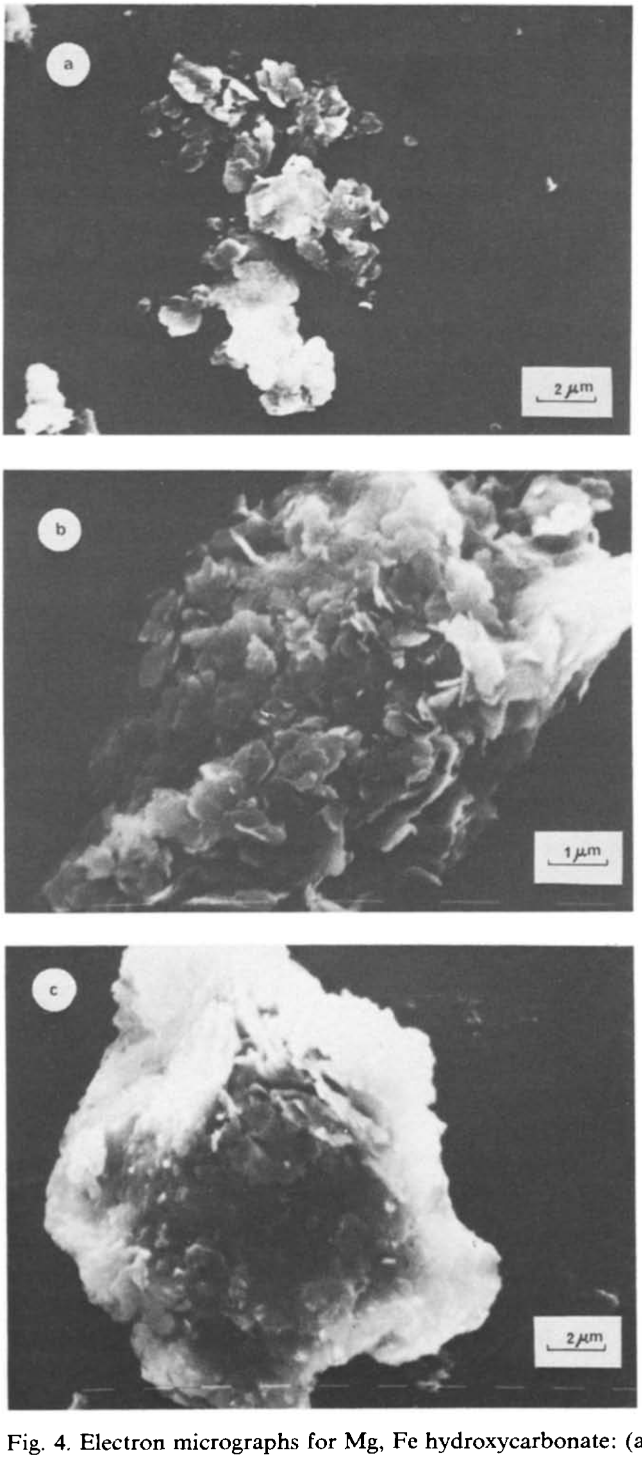

Fig. 4. Electron micrographs for Mg, Fe hydroxycarbonate: (a) 25 °C; (b) 600 °C; (c) 975 °C.

TABLE 1

Results of N_2 adsorption at 77 K of undecomposed and thermally treated synthetic pyroaurite

T (°C)	S_{BET}	S_{α}	S_{cum}	S'_{cum}	V_p (ml g^{-1})
	(m^2 g^{-1})				
25	48.2	49.0	45.3	27.5	0.1440
150	48.8	49.1	46.0	30.1	0.1520
240	49.3	49.5	47.5	31.9	0.1680
440	53.8	54.1	50.2	38.5	0.2000
600	60.6	62.3	55.6	40.2	0.2432
800	52.0	51.8	47.3	37.3	0.1920
975	15.6	15.5	–	–	0.0512

indicates that the pore shape of these samples can be explained by assuming a cylindrical (or interstices between close-packed particles) geometry according to the Dollimore and Heal calculation [14]. On increasing temperature, dehydration takes place and the BET surface area increases slowly. However, the original plate-morphology with a distinct hexagonal outline (Fig. 4a), which resembles that obtained for a hydrotalcite-like compound [20], did not change appreciably. When the original sample is heated to a temperature above the second endothermic peak, the BET surface area reaches the maximum value. It is consistent with the formation of a mixture of MgO and the spinel $MgFe_2O_4$ and corroborated by the SEM micrograph (Fig. 4b) showing agglomerates of small particles of fairly uniform size. At higher temperatures (975 °C) the specific surface area drastically disminishes because of sinterization of the sample and the disappearance of its mesoporosity, as is observed in the SEM micrograph of Fig. 4c. The V_p values obtained for samples studied (Table 1) are directly correlated with the corresponding BET surface areas.

REFERENCES

1 H.F.W. Taylor, Mineral. Mag., 39 (1973) 377.
2 S. Miyata, Clays Clay Miner., 23 (1975) 369.
3 S. Miyata and T. Kumura, Chem. Lett., (1973) 843.
4 R. Allmann, Chimia, 24 (1970) 99.
5 G.W. Brindley and S. Kikkawa, Clays Clay Miner., 28 (1980) 87.
6 S. Miyata, Clays Clay Miner., 28 (1980) 50.
7 O. Marino and G. Mascolo, Thermochim. Acta, 55 (1982) 377.
8 M.J. Hernandez, M.A. Ulibarri, J.L. Rendon and C.J. Serna, Thermochim. Acta, 81 (1984) 311.
9 K. Hashi, S. Kikawa and M. Koizumi, Clays Clay Miner., 31 (1983) 152.
10 S. Miyata and T. Hirose, Clays Clay Miner., 28 (1980) 87.
11 M.A. Ulibarri, M.J. Hernandez and J. Cornejo, Mat. Chem. Phys., 14 (1986) 209.

12 S. Brunauer, P.H. Emmett and E. Teller, J. Am. Chem. Soc., 60 (1938) 309.
13 K.S.W. Sing, in D.H. Everett and R.H. Ottewill (Eds.), Surface Area Determination, Proceedings of International Symposium, Butterworths, London, 1969, p. 25.
14 D. Dollimore and G.R. Heal, J. Colloid Interface Sci., 33 (1970) 508.
15 B.C. Lippens, B.G. Linsen and J.H. de Boer, J. Catal., 3 (1964) 32.
16 R. Allmann, Acta Crystallogr., Part B, 24 (1968) 972.
17 P.G. Rouxhet and H.F.W. Taylor, Chimia, 23 (1969) 480.
18 S. Brunauer, L.S. Deming, W.F. Deming and E. Teller, J. Am. Chem. Soc., 62 (1940) 1723.
19 IUPAC, Pure Appl. Chem., 57 (1985) 603.
20 M.A. Ulibarri, M.J. Hernandez, J. Cornejo and C.J. Serna, Mat. Chem. Phys., 14 (1986) 569.